JOURNAL OF MATERIALS SCIENCE 29 (1994) 250–254

Microstructural features of sintered Si_3N_4/SiC-whiskers composites: mechanical integrity of whiskers

M. E. BRITO*, Y. BANDO, M. MITOMO
National Institute for Research in Inorganic Materials, Namiki 1-1, Tsukuba, Ibaraki 305, Japan

S. SAITO
Japan Metals and Chemicals Co., 1-4-63 Ohama, Sakata, Yamagata 998, Japan

A detailed microstructural analysis of slip-cast Si_3N_4/SiC-whisker composites has been made by TEM. In spite of the gentle forming process, SiC whisker breakage constitutes a fundamental feature of this material. The breaking takes place during the sintering process and could be associated with residual thermal stresses, as revealed by the experimental evidence. The dramatic decrease in the whiskers aspect ratio translates into little or no effect of whisker addition on the mechanical properties of the Si_3N_4 matrix.

1. Introduction

The use of silicon carbide (SiC) whiskers as reinforcement for monolithic structural ceramics is becoming a common technology in the search for strong and tough ceramics. The most important factors for selecting SiC whiskers for the reinforcement of ceramics are: (1) geometrical factors, e.g. shape, size, aspect ratio; (2) their chemical stability; and (3) their compatibility in physical properties with several ceramics matrices, e.g. thermal expansion coefficients. In particular, composites consisting of SiC whiskers in silicon nitride (Si_3N_4) matrices are reported to present an increase in room-temperature fracture toughness and strength [1, 2]; however, expectations of increases of fracture toughness values as large as those obtained for alumina or mullite [3, 4], have not been fulfilled. No clear reason has yet been proposed for this behaviour.

The proposed major toughening mechanisms for this type of materials are crack deflection [5], crack bridging and whisker pull-out [6, 7]. Because the surface characteristics of whiskers play an important role in all these toughening mechanisms, most of the microstructural characterization work has been undertaken to understand the behaviour and development of whisker–matrix interfaces [8, 9]. However, the effectiveness of whiskers is greatly affected by the geometrical factors mentioned above and therefore morphological integrity of whiskers during composites manufacturing is an important matter to be addressed. Preserving, as much as possible, the original geometry of whiskers during processing is considered of vital importance to make whisker addition worthwhile.

Processing techniques used to consolidate SiC(w)–Si_3N_4 composites, such as hot-pressing [7] or hot isostatic pressing (HIP) [10] preceded by mixing of raw materials in a ball mill, induce irreparable damage on the whiskers. In contrast, slip-casting offers a more gentle manner to process this type of material. Mitomo *et al.* [11] have succeeded in sintering highly oriented Si_3N_4/SiC whisker composites through a combination of slip-casting and pressureless sintering techniques. They reported the sintering anisotropy of the composite and a slight anisotropy in fracture toughness when a crack propagated perpendicular to the slip direction. Optical microscopy of polished surfaces indicated alignment of whiskers in the slip direction. However, considering the apparent anisotropy of the microstructure, no proportional and clear effect on the material toughness could be observed. In this preliminary microstructural study of slip-cast Si_3N_4/SiC composites, we have stressed the significance of morphological integrity that the whiskers possess in the toughening of structural ceramics.

2. Experimental procedure

Si_3N_4 powders (8S grade, Japan Metals and Chemicals Co., Japan), SiC whiskers (TWS 100 grade, Tokai Carbon Co., Japan), sintering additives and a deflocculant were mixed for 46 h in deionized water using an alumina ball mill. The amount of SiC whiskers was 10 wt %. Sintering additives were 8 wt % Y_2O_3 (99.99 % pure, Shin-etsu Chemical Co., Japan), 5 wt % Al_2O_3 (AKP-30 grade, Sumitomo Chemical Co., Japan) and 2% cordierite ($Mg_2Al_4Si_5O_{18}$, SS600 grade, Marusu Yuyaku Co., Japan). The slurry so obtained with a solid content of about 70 wt % was cast and dried. Green bodies were then pressureless

Present address: National Industrial Research Institute of Nagoya, Hirate 1-1, Nagoya, Aichi 462, Japan.

0022–2461 © *1994 Chapman & Hall*

sintered at 1750 °C for 1 h, in a nitrogen atmosphere. Details of the processing method are given elsewhere [11].

The fracture toughness, K_{Ic}, was measured by the micro-indentation method [12] under 10 kg load for sections parallel and perpendicular to the slip axis. A maximum value of up to 6 MN $m^{-3/2}$ for crack propagation on the slip plane perpendicular to the slip direction was obtained, while no appreciable change with respect to the matrix (about 4.5 MN $m^{-3/2}$) was observed for crack propagation in the cross-sectional plane to the slip direction [11]. Thin sections were cut from the sample both parallel and perpendicular to the slip axis for transmission electron microscopy (TEM) observation. The sections were mechanically polished to approximately 50 μm, dimpled, and ion milled to electron transparency. The accelerating voltage and beam-current conditions for ion milling were, respectively, 6 kV and 0.8 mA at 20° gun tilt until perforation, and finishing at 3 kV and 0.6 mA at 10° to remove surface damage produced during milling at the higher voltage. Whisker morphology in the as-received condition was also analysed by TEM. Conventional TEM, as well as high-resolution electron microscopy (HRTEM) were performed using a JEM-2000EX operated at 200 kV.

3. Results and discussion

3.1. Whisker morphology

The faulty structure of whiskers is revealed by the transmission electron micrographs of Fig. 1. Whiskers presenting different morphologies in the as-received condition (Fig. 1a and b) are present within the same product grade, indicating that different whisker growth conditions take place. Whiskers composed of segments, such as that on the right-hand side of Fig. 1b, will be subject to further analysis later in the paper. No particular attempt was conducted to determine quantitatively the distribution by morphology of whiskers. However, it is reasonable to assume that the response of each particular type of whisker to thermal and mechanical treatment could be different.

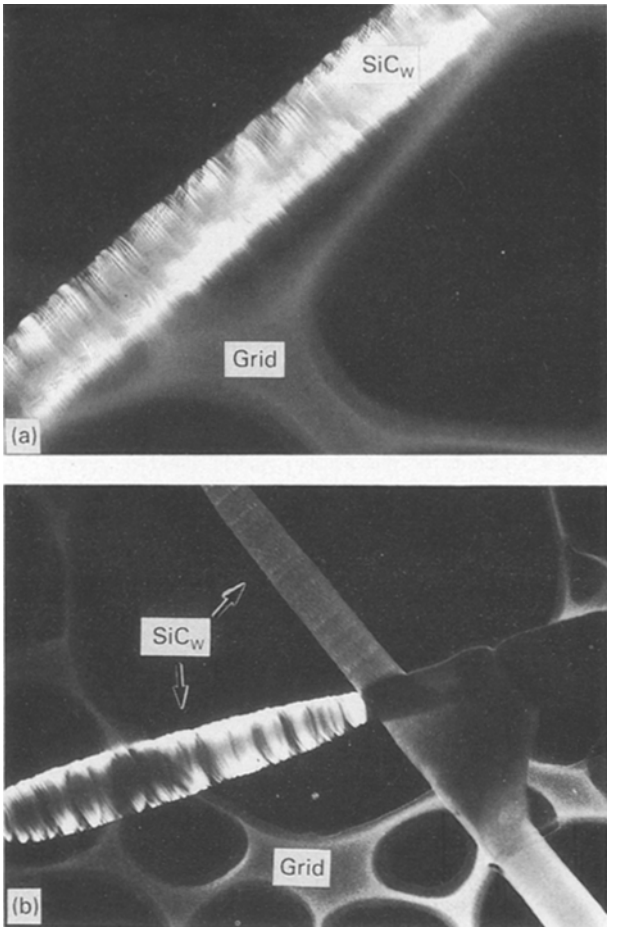

Figure 1 Morphological features of SiC whiskers in the as-received condition.

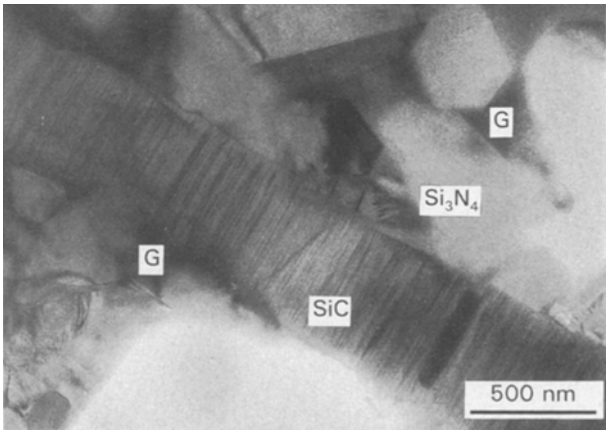

Figure 2 Low-magnification transmission electron micrograph showing the composite microstructure.

3.2. Sintered body microstructure

A low-magnification TEM image of the sintered body microstructure is shown in Fig. 2. β-Si_3N_4 grains having a grain size ranging between 0.2 and 1 μm, SiC whiskers, and an amorphous phase (G in the micrograph) occurring along the matrix grain boundaries and at grain junction, can be observed. Owing to the low volume fraction of whiskers, only one or two of them can be observed within the same micrograph area. Although macroscopic analysis of the microstructure reveals a high degree of directionality parallel to the slip axis, no appreciable change was found in the local structure when comparing sections transverse and parallel to the slip axis. That is, many unaligned whiskers can be observed within the matrix.

Details of the whisker–matrix interface region can be seen in the micrograph of Fig. 3. β-Si_3N_4 grains of several tens of nanometres in size, indicated by arrows in the figure, present clear facets forming interfaces with the SiC whisker. Pockets of a glassy phase can also be observed in contact with the whisker surface.

At the matrix–whisker interface, two prominent features could be observed by means of HRTEM. Fig. 4 shows the case where no third phase exists at the interface between the whiskers and the Si_3N_4 matrix. The micrograph reveals a topotactic crystallographic relationship at the interface. In the micrograph, SiC is viewed with the electron beam parallel to $\langle 1\,1\,0 \rangle$ while $h\,0\,0$ fringes of Si_3N_4, taken several degrees tilted from

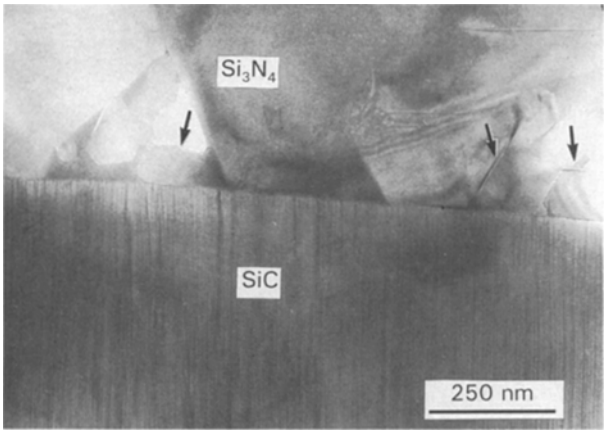

Figure 3 Details of the whisker–matrix interface region. The amorphous phase in contact with the whisker is evident in pockets at multi-grain junctions.

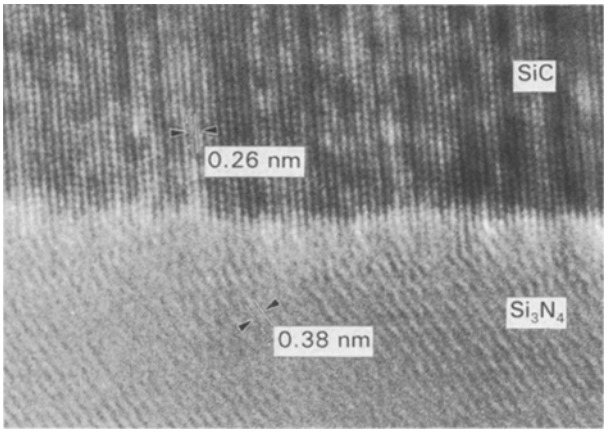

Figure 4 High-resolution transmission electron micrograph of the interface between an Si_3N_4 grain and the SiC whisker. Total absence of a third phase and a topotactic crystallographic relationship at the interface are the most important features.

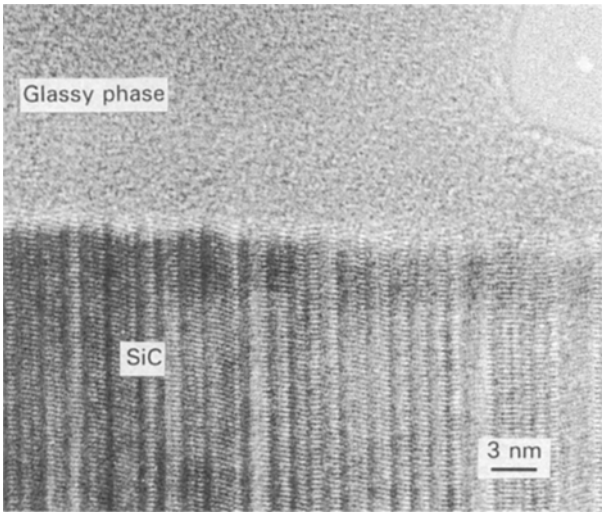

Figure 5 High-resolution transmission electron micrograph of the interface between a pocket of glassy phase and the SiC whisker.

the ⟨001⟩ direction, run up to the interface. Si_3N_4 grains, possibly grew using clean portions of the SiC as substrate, give an origin to this type of clean interface. However, depending on the local amount of glassy phase, matrix–whisker interfaces with an amorphous layer as buffer in between, seem to be the most common feature. Furthermore, as mentioned before, large grains junction pockets filled with a glassy phase are in contact with the whisker surfaces, like that observed in the HRTEM image of Fig. 5. This suggests that most whiskers are embedded in such a phase. No evidence for dissolution of whiskers in the glassy phase was found and no attempt was undertaken to determine the chemical composition of the glassy phase.

Fig. 6 represents a micrograph pair of bright-field (Fig. 6a) and dark-field images (Fig. 6b) showing an area where, coincidentally, two whiskers lay beside each other. The original faulty structure of the whiskers makes them easily distinguishable within the structure. Depending on its orientation with respect to the incident electron beam, a clear contrast generated by stacking faults (W1 in Fig. 6a) and/or dislocation (W2 in Fig. 6a) is observable. The dark-field image of Fig. 6b provides the clearest aspect of the whiskers faulty structure. Segmentation of the image corresponding to W1 is clearly observed, while complex Moiré patterns due to interactions of dislocations, planar defects and thickness fringes, are depicted for whisker W2.

As confirmed by the electron diffraction analysis, the whiskers present a ⟨111⟩ growth direction with a structure that alternates segments of β-SiC single crystal (Fig. 7a) with segments exhibiting a high density of planar defects (Fig. 7b). It is using the crystallographic

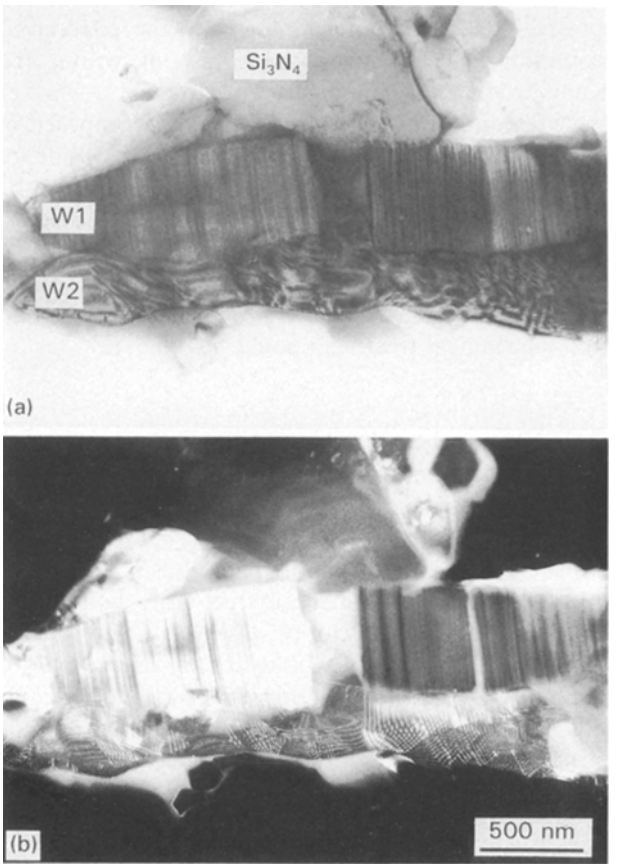

Figure 6 (a) Bright-field and (b) dark-field micrographs of a couple of whiskers lying together. Notice the characteristic contrast for stacking faults formation for the whisker oriented parallel to ⟨110⟩ with respect to the electron beam (upper part).

orientation of Fig. 7, ⟨110⟩ zone axis, that the whiskers exhibit the characteristic contrast observed for whisker W1 of Fig. 6a. The same morphology for SiC whiskers was observed in a recent characterization work by Wang *et al.* [13]. Along the ⟨110⟩ zone axis, the single-phase segment exhibits a change in diameter. Wang *et al.* have explained this observation in terms of the tendency to develop non-basal {111} surfaces during growth, resulting in the formation of crystals resembling truncated pyramids of triangular section. Once the growing β-SiC single crystal reaches an energetically critical diameter, stacking faults develop to reduce the overall energy [13]. Successively, when given conditions (supersaturation, etc.) to grow β-phase are newly reached, another segment is formed trapped in between faulted segments, as in Fig. 6a.

Segmentation of a whisker during growth also affects its cross-sectional appearance. The faulted segments consist basically of α-phase polytypes which form, introducing 180° rotational twins periodically into the β-phase structure, generating hexagonal or rhombohedral stacking sequences [14, 15]. From there, every change in the structure along the whisker is accompanied by a change from a triangular cross-section to a hexagonal one. The implications that this type of morphology has on the role that whiskers might play in improving mechanical properties of monolithic ceramics are evident. Pronounced changes in cross-section translate into notched whisker surfaces and in turn into weak points along the whisker.

3.6. Whisker breakage

The most intriguing fact during the analysis of specimens microstructures was the high density of fractured whiskers, as shown in Fig. 8. The whisker presents a fracture parallel to the basal (111) plane and specifically in the region where the structure changes from the β-SiC segment to the planar faulted segment. It is important to notice that this fracture type, where only a narrow gap between segments is produced, would not affect the whisker appearance when observed at low magnification using optical electron microscopy or scanning electron microscopy (SEM).

Thermal expansion and thermal expansion anisotropy of the crystal depend on structural factors such as the strength of bonds within each of the structural

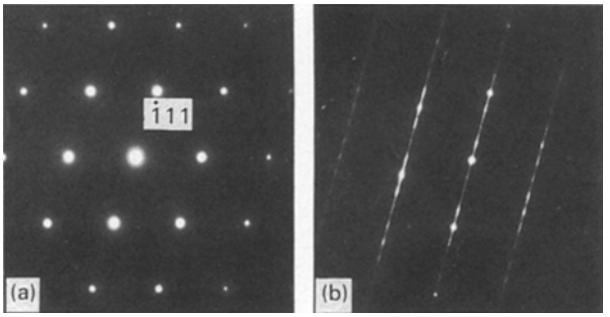

Figure 7 Diffraction patterns for the β-phase single-crystal segment and the faulted segment of the SiC whisker.

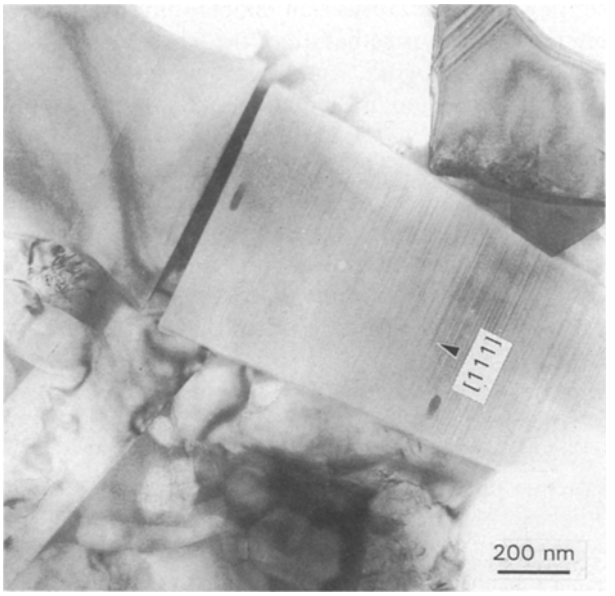

Figure 8 Whisker spontaneously fractured at the region limiting a single crystal and faulty segments.

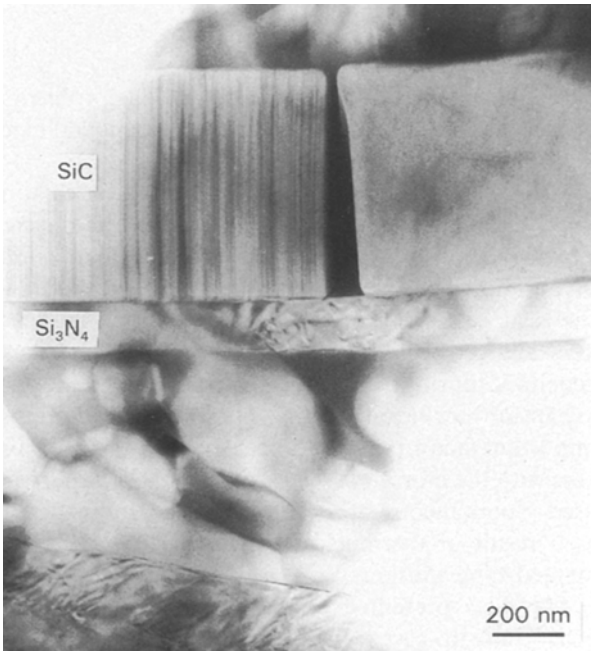

Figure 9 Whisker showing fracture. Notice the strong strain contrast due to plastic deformation of the neighbouring Si_3N_4 grain in the middle of the figure.

polyhedra and the angular changes between the polyhedra [16] and coefficients of thermal expansion for crystalline structures should consist of a combination of these two factors. It is reasonable to assume that at the interface between a single-crystal β-SiC segment and a faulted segment, residual stresses were generated and produce spontaneous breakage of whiskers in the fashion shown in Fig. 8. Li and Bradt [17] have analysed thermal expansion and elastic anisotropies of SiC in relation to its polytype structure. They pointed out that a single crystal constituted of ideal whiskers grown in the ⟨111⟩ crystallographic direction develop the largest thermoelastic residual stresses on

cooling from the fabrication temperatures. Considering the segment-type nature of the whiskers analysed in the present work, and the slight differences in thermal expansion mismatch between β-phase and α-phase, $5.1 \times 10^{-6}\,°C^{-1}$ and $4.8 \times 10^{-6}\,°C^{-1}$ at 1000 °C, respectively [17], a clear explanation is depicted for spontaneous breakage of whiskers due to intrinsic factors during the sintering process. Needless to say, it is also important to consider the thermoelastic characteristic of the matrix.

Fig. 9 shows another whisker that fractured similarly at the boundary of two segments. However, an important detail can be observed: plastic deformation, evinced by the high strain contrast, induced by the fractured whisker upon the neighbouring Si_3N_4 grain. Fracture takes place at relatively lower temperatures, otherwise the strain within the Si_3N_4 grain could be relieved [18]. This type of fracture, where the gap generated between the fractured parts is wide and deformation in surrounding areas is observed, is more likely to be associated with thermal stresses generated between the SiC whisker and the matrix or the surrounding amorphous phase.

4. Conclusion

Although a quantitative description of the problem is not affordable at the moment, the experimental evidence may be summarized as follows.

Upon cooling from the sintering temperature, relatively high thermal stresses, generated by thermal expansion mismatch between whisker–amorphous phase and whisker–matrix, arise, inducing fracture in the weak sections of whiskers. Considering that whiskers are generally soaked in the amorphous phase generated during sintering, it is perhaps the thermal expansion coefficient of this phase that is the most important factor that should be controlled when whiskers with the morphologies discussed in this report are used. Spontaneous breakage of whiskers also occurs as a result of thermoelastic mismatch between segmented-type whiskers.

The facts presented above, would contradict our belief that slip-cast techniques reduce by a great deal the mechanical damage induced in whiskers using other forming techniques. Because the aspect ratio of whiskers has the largest influence on toughening by crack deflection in whisker-reinforced composites [19], the fracture and sectioning of whiskers during processing reduce greatly their effectiveness. In the same way, considering that the diameter of whiskers has the largest effect on fracture toughness, referring to the crack-bridging mechanism [20], whiskers presenting weak points along their axis are not useful to arrest cracks propagating within ceramic matrices. The poor morphological integrity of whiskers used in the preparation of our specimen explains well the low fracture toughness values for our specimen, independently of the apparent isotropic character of its microstructure. The direct implication and generality of our results can be appreciated in a recent work by Choi and Salem [21] who claim that whisker addition to Si_3N_4 ceramics does not impart any favourable effects on strength and fracture toughness. Their results are in clear contradiction with those reported elsewhere [1, 2], where increase in fracture toughness and strength is claimed for Si_3N_4–SiC whiskers composites.

References

1. P. D. SHALEK, J. J. PETROVIC, G. F. HURLEY and F. D. GAC, *Am. Ceram. Soc. Bull.* **65** (1986) 351.
2. S. T. BULJAN, J. G. BALDONI and M. L. HUCKABEE, *ibid.* **66** (1987) 347.
3. T. N. NIEGS and P. F. BECHER, *ibid.* **66** (1987) 339.
4. G. C. WEI and P. F. BECHER, *ibid.* **64** (1985) 298.
5. M. R. RUEHLE, B. O. DALGLEISH and A. G. EVANS, *Scripta Metall.* **21** (1987) 681.
6. A. G. EVANS, *Acta Metall.* **34** (1986) 2435.
7. S. V. NAIR, *J. Am. Ceram. Soc.* **73** (1990) 2839.
8. S. A. BRADLEY, K. R. KARASEK, M. R. MARTIN, H. C. YEH and J. L. SCHIENLE, *ibid.* **72** (1989) 628.
9. W. BRAUE, R. W. CARPENTER and D. J. SMITH, *J. Mater. Sci.* **25** (1990) 2949.
10. G. PEZZOTTI, I. TANAKA, T. OKAMOTO, *J. Am. Ceram. Soc.* **73** (1990) 3033.
11. M. MITOMO, S. SAITO, T. MATSUDA and T. YONEZAWA, *J. Mater. Sci.*, to be published.
12. A. G. EVANS and E. A. CHARLES, *J. Am. Ceram. Soc.* **59** (1976) 371.
13. L. WANG, H. WADA and L. F. ALLARD, *J. Mater. Res.* **7** (1992) 155.
14. L. RAMSDELL, *Am. Mineral.* **18** (1947) 64.
15. W. F. KNIPPENBERG, *Phillips Res. Rep.* (1963) 161.
16. H. D. MEGAW, *Mater. Res. Bull.* **8** (1971) 1007.
17. Z. LI and R. C. BRADT, in "Proceedings of the Silicon Carbide 1987 Symposium", Columbus, August 1987, edited by J. D. Cawley and C. E. Semler (The American Ceramic Society, Westerville, 1989) p. 313.
18. W. F. LEE and G. E. HILMAN, *J. Am. Ceram. Soc.* **72** (1989) 1931.
19. K. T. FABER and A. G. EVANS, *Acta Metall.* **31** (1983) 565.
20. P. F. BECHER, *J. Am. Ceram. Soc.* **74** (1991) 255.
21. S. R. CHOI and J. A. SALEM, *J. Mater. Sci.* **27** (1992) 1491.

Received 25 February
and accepted 27 April 1993